Module 5: Schlieren and Shadowgraph

Lecture 31: Results and discussion related to crystal growth (part 1)

The Lecture Contains:

Previous Next

CONVECTION PHENOMENA DURING CRYSTAL GROWTH

For a purely buoyancy-driven growth process, the driving potential of flow is the maximum concentration difference occurring in the solution. In addition, the strength of convection is also governed by the length scale, typically the size of the growing crystal. With time, the solution is depleted of the salt, though there is an increase in the length scale related to the change in size of the crystal. Jointly, the strength of convection can increase with time, till the solution in the growth chamber is fully depleted of salt. This state is characterized by stable stratification of the solution, the convection currents diminishing in strength to negligible levels. The growth of the crystal practically stops at this stage. Growth can be resumed when the grown crystal is immersed in a fresh supersaturated solution and the ramp rates are re-introduced. The resulting convection patterns would be different from the first stage because of a change in the crystal size. When the crystal is imparted rotation, velocities are created in the angular direction in the horizontal plane, in addition to the buoyancy-driven motion in the vertical plane. However, the two motions are interlinked through the radial component of velocity. The linkage is such that rotational motion leads to Coriolis forces that re-direct fluid motion. However, homogenization of the solution is the dominant factor that reduces concentration gradients, diminishes the driving potential and hence suppresses fluid motion arising from buoyancy. The critical speed at which buoyancy is practically suppressed will depend on the crystal size and overall concentration difference available in the solution. The resulting solutal concentration distribution at the surface of the crystal influences the growth rate and quality.

The process of solute deposition leading to crystal growth occurs on a hierarchy of length and time scales. At the small scale, solute particles arrange themselves as a part of the crystal structure. The pyramidal structure seen at later stages of growth is initiated at this point. The experiments conducted in the present work do not yield information on this aspect of the growth process. At the larger scale (the length scale of the crystal itself), concentration gradients are set up that feed solute to the crystal. These gradients naturally control the rate of crystal growth. The uniformity in distribution of the concentration gradients determines the crystal quality. The present research aims at investigating physical mechanisms at the scale of the crystal in terms of the solutal concentration distribution.

Previous Next

COMPARISON OF INTERFEROMETRY, SCHLIEREN AND SHADOW-GRAPH IN A CRYSTAL GROWTH EXPERIMENT

The applications of interferometry, schlieren and shadowgraph as tools for visualization of buoyant convection and on-line monitoring of KDP crystal growth from its aqueous solution are discussed in the present section. The ramp rate here is around $0.2\ ^{\circ}C/hour$ that is quite high in comparison to the rates employed in Section Influence of Ramp Rate and Crystal Rotation on Convection Patterns of the present lecture. The resulting convection patterns, as a result, form earlier in the experiments discussed. Images of the time-evolution of the convective field in the growth chamber have been recorded. The three measurement techniques are compared in terms of image quality and the potential for extracting quantitative information.

CONVECTION PATTERNS

When a seed of the crystal is inserted in the solution, the initial temperature difference between the two leads to the dissolution of the seed itself. The local density of the solution increases, and consequently the solution descends vertically from the crystal. With the passage of time, thermal equilibrium is established, and density differences within the solution are solely due to concentration differences. Adjacent to the crystal, the solute deposits on the crystal faces, and the solution goes from the supersaturated to the saturated state. Thus the solution near the crystal is lighter than the solution away from it. The denser solution displaces the lighter fluid, and a circulation pattern is set up around the crystal. The structured movement of the fluid, called a buoyant plume is essential for transporting the solute from the bulk of the solution to the crystal and determines the crystal growth rate. The plume is visible in the three visualization techniques: as fringe displacement in interferometry, and the spread of light intensity in schlieren and shadowgraph.

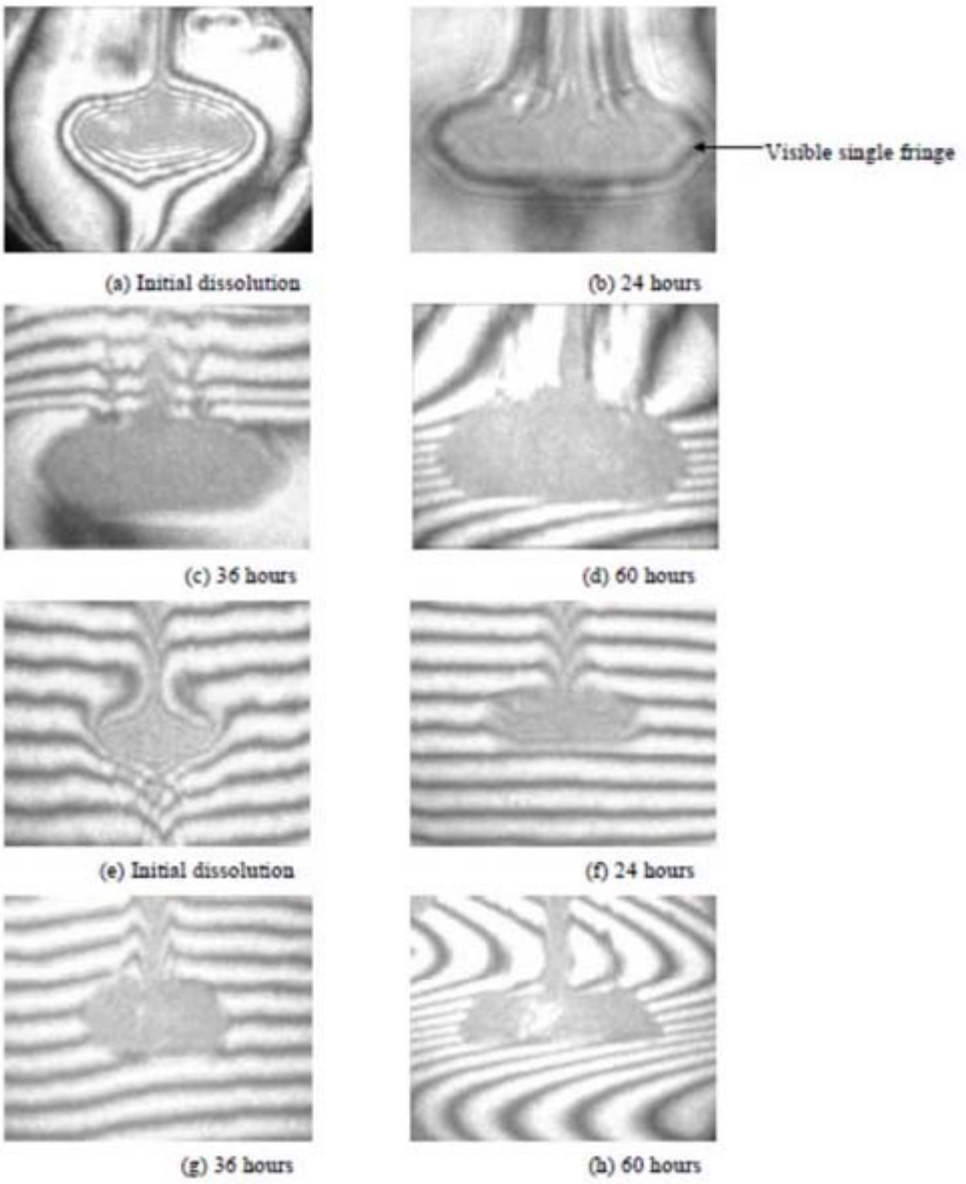

Figure 5.16: Time sequence of the evolution of interferograms around the growing crystal. (a-d) Infinite Fringe setting; (e-h) Wedge fringe setting. The initial crystal size in the infinite fringe setting is greater than in the wedge fringe setting. Large fringe slopes in (e-h) very close to the glass rod are possibly distortions. The opposing fringe curvatures above and below the crystal in (h) show a lighter and a denser solution formed by stratification

Previous Next

Figure 5.16 shows the formation and time-evolution of fringes in the infinite and wedge fringe settings of the interferometer around the growing crystal. The first image of the transient shows the appearance of fringes due to crystal dissolution. This process increases the local density, causing the solution to descend vertically downwards. Hence, the fringe displacement is also in the downward direction (Figure 5.16(a)). Large concentration gradients in the vicinity of the dissolving crystal give rise to time-dependent fluid motion as well. A second factor contributing to unsteadiness is the change in the crystal geometry from rectangular to prismatic. As the crystal attains thermal equilibrium on one hand and its natural shape on the other, the concentration gradients gradually diminish. During a time period of 15-35 hours, the gradients were small enough to produce only a single visible fringe adjacent to the growing crystal (Figure 5.16(b)). The fringe was found to be stable with respect to time indicating uniform deposition of the solute around the growing crystal. Experiments in the wedge fringe setting of the interferometer reflect identical trends. The horizontal fringes deform vertically downwards (Figure 5.16(e-f)), and is followed by a phase when they are practically straight. Near the crystal, the solution is practically saturated, while it is supersaturated in the far field. The wedge fringes get displaced in regions of a large change in concentration with respect to the bulk of the supersaturated solution. With further cooling, the solution in the near-field becomes supersaturated with reference to the new temperature, additional salt deposits on the crystal, and the growth process is once again initiated. This leads to concentration gradients adjacent to the crystal, and a continuation of buoyancy-driven flow. In the time frame of 20-30 hours after the insertion of the KDP seed, the infinite and the wedge fringes showed considerable symmetry as well as stability in time, ensuring uniform growth on all the faces of the crystal. This time duration may be called the stable growth regime of the crystal.

With an increase in the crystal size, the influence of even mild concentration gradients is strengthened, increasing the fringe deformation. Over a longer duration of the experimental run time (> 50 hours), the solution is found to be layered (stratified) with respect to density (Figures 5.16(c-d) in the infinite fringe setting and Figures 5.16(g-h) in the wedge fringe setting). This is understandable because crystal growth takes place from a fixed volume of the solution in the growth chamber, and with time, the solution is increasingly depleted of salt. The density inversion suppresses convection to a point where the increase in the crystal size is negligible. The downward movement of these layers of constant concentration is driven by molecular diffusion, and contributes to a very slow increase in the crystal size. The appearance of straight horizontal fringes above the crystal in the infinite fringe setting, and opposed curvature of wedge fringes in the far-field can thus be taken as the limiting point where the growth process is to be terminated.

Previous Next

The initial size of the crystal used in the infinite fringe setting had to be larger than that of wedge fringes. This is because the convection patterns with a small crystal did not produce sufficient contrast in the interferograms, and could be recorded by the camera.

The growth sequence using schlieren and shadowgraph techniques is shown in detail in Figures 5.17 and 5.18. They confirm the evolution pattern of the convection field recorded by the interferometer. The first image in the schlieren and shadowgraph sequences shows initial dissolution of the seed just after its insertion into the solution. A sharp descending plume originating from the seed can be seen. The intensity contrast is related to an abrupt change in the solute concentration around the seed crystal, which creates a jump in the refractive index, and deflects the light beam into the region of relatively large concentration gradients. The schlieren arrangement is more sensitive to the change in concentration, producing a greater intensity contrast, when compared to the shadowgraph. After the initial dissolution, the growth process of the crystal is initiated. The associated convection currents are larger, and a significant increase in the size of the bright region is seen. The schlieren image is more vivid (Figure 5.17), when compared to the shadowgraph (Figure 5.18). The images also reveal the extent of symmetry of the solutal distribution and the underlying flow field in the stable growth regime of the crystal. As in interferograms, schlieren and shadowgraph reveal the following sequence of events: (a) The plumes associated with crystal dissolution are unsteady; (b) the growth process enters a stable growth regime till the crystal size exceeds a critical value; and (c) the flow field approaches a stagnant condition when the solution becomes stratified.

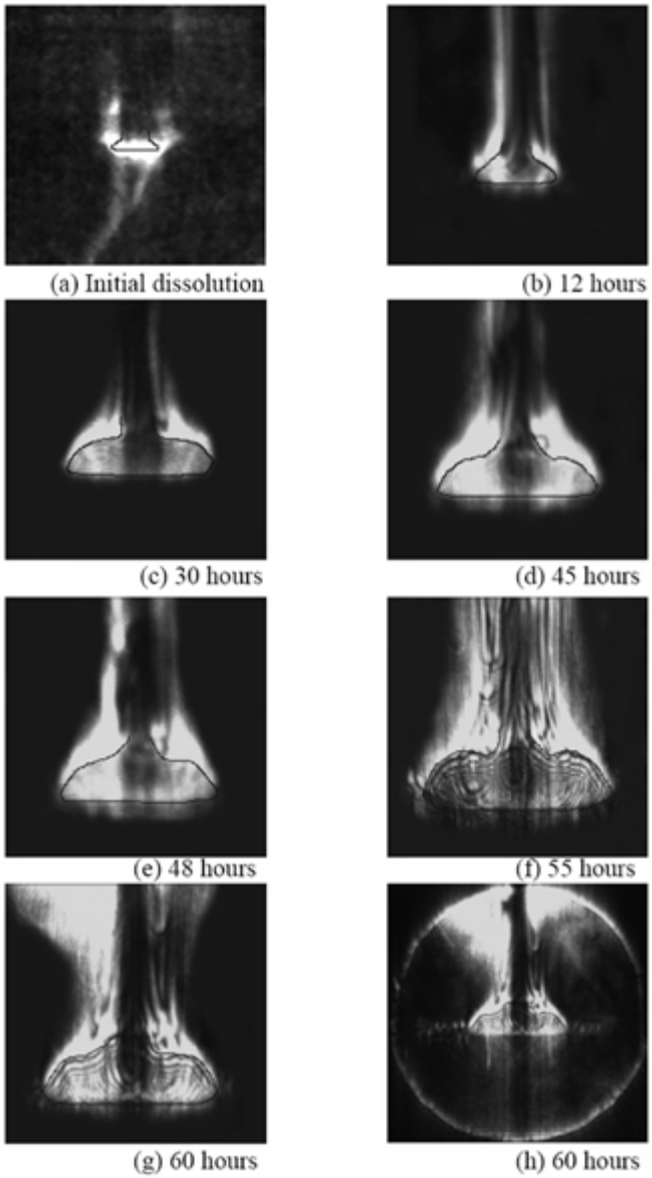

Figure 5.17: Evolution of schlieren images around the growing crystal from an aqueous solution. Images have been contrast-enhanced to reveal clearly the regions of high brightness. In (h) the original photograph as recorded by the camera is shown. The crystal position has been highlighted.

Previous Next

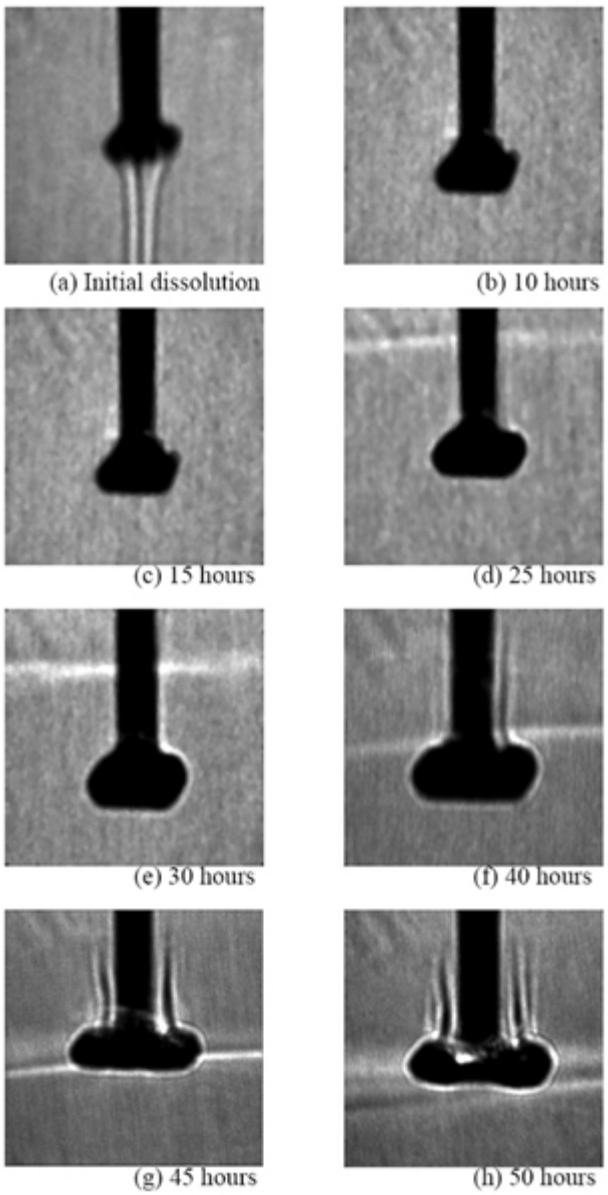

Figure 5.18: Evolution of shadowgraph images around the growing crystal from an aqeous solution. Images have been contrast-improved for clarity. A bright streak of light indicates the separation of the light solution from the heavy. The streak is seen to move downwards in (d-h), till it stablizes just around the crystal.

Previous Next

The layering and stable stratification of the solution are seen for times greater than 55 hours (Figures 5.17(g-h) and Figures 5.18(g-h)). In the schlieren image, it leads to the region of brightness shifting away from the crystal. Figure 5.17(h) is an original unprocessed schlieren image. It shows a larger view of convection around the crystal, where stratification leads to a significant refraction and the appearance of a bright patch of light above the crystal. In shadowgraph images, the movement of the stratification front is visible as a bright band that descends vertically downwards. For times greater than 50 hours, the patch of light is localized around the crystal, while alternating bands of bright and dark regions are formed.

The schlieren (Figures 5.17(c-d)) and shadowgraph images (Figure 5.18(e-f)) in the stable growth regime show an upward movement of the buoyant plumes around the crystal. These plumes end in the bulk of the solution in the beaker, and descend in such a way as to form a closed loop. The images discussed in the present section pertain to the flow field adjacent to the crystal alone. The buoyant plumes in the stable growth regime are responsible for the deposition of the solute on the crystal surface. These convection plumes are almost steady and uniform in nature resulting in uniform and symmetric growth of the crystal. The gradient of concentration is larger near the crystal surface when compared to the bulk of the solution. This distribution can be visualized as a diffusion boundary layer around the growing faces of the crystal. The thickness of the boundary-layer can be identified as the region over which the light intensity is high. The vertically upward movement of the convective plumes results in the variation of the thickness of concentration boundary layer along the crystal faces. During the growth phase of the crystal, the boundary-layer is the thinnest on the lower side of the crystal, and the highest on the upper side.
The shadowgraph images are not as explicit as the schlieren, but they help in deciding the symmetry pattern of growth, time dependence, and the onset of stratification. It is to be expected that the shadowgraph images would show greater contrast when the gradients are very high, for example crystal growth in forced convection conditions.

Previous Next

COMPARISON OF THE THREE TECHNIQUES

The knowledge of transport phenomena in the growth of crystals from their aqueous solution in the free convection regime is important for understanding the fundamental mechanisms involved and for fixing process parameters. As opposed to forced convection, the free convection technique has its own importance, for example in protein crystal growth where it is the only choice because of its delicate structure and the ease of managing defects. The creation of a homogeneous concentration field in the boundary-layer adjacent to the solution-crystal interface and uniform distribution of solute in the bulk solution are two major requirements. Refractive index-based optical techniques can be used to examine the nature of convection patterns as a function of time and hence the quality of the grown crystal.

A comparison of the images of the three techniques shows interferograms to be most vivid, since fringes deform and get displaced in relationship to the local velocity field. Thus, they offer the most direct information about concentration distribution as well as the underlying flow field in the solution. Schlieren and shadowgraph images reveal regions of high concentration gradients in the form of heightened brightness, though the former shows greater sensitivity. A review of Equations 1, 3 and 5 shows that interferograms are easy to analyze, schlieren requires integration of the intensity field, (Lecture 29) while shadowgraph requires the solution of a Poisson equation to recover the local concentration.

The three optical techniques under discussion yield images that are integrated values of the concentration field in the direction of propagation of the light beam. Thus, if the spatial extent of the disturbed zone in the solution is small, the information contained in the image is small. In the context of interferometry, the consequence could be the appearance of too few fringes in the infinite fringe setting and small fringe deformation in the wedge fringe setting. In schlieren and shadowgraph, weak disturbances show up as small changes in intensity and hence contrast. The difficulty can be alleviated in schlieren by using large focal length optics so that small deflections are amplified. In shadowgraph, image quality can be improved by moving the screen away from the test cell. Additional difficulties with interferometry are the need for maintaining identical experimental conditions in the crystal growth and the compensation chambers, careful balancing of the test and the reference beams, and limitations arising from fact that quantitative information is localized at the fringes. This discussion shows that configuring the interferometer as the instrument for on-line process control poses the greatest challenge, schlieren and shadowgraph being relatively simpler. Based on the above discussion, schlieren may be considered as an optimum while comparing the ease of analysis with the difficulty of instrumentation.

Previous Next

INFLUENCE OF RAMP RATE AND CRYSTAL ROTATION ON CONVECTION PATTERNS

The present section discusses the application of the laser schlieren technique to monitoring convection in a crystal growth process from its aqueous solution, when the process parameters are varied. The cooling rate of the solution determines the amount of excess salt available in the solution for deposition on the crystal, and hence the potential difference for driving the convection currents. Ramp rates of 0.05 and $0.1°C/hour$ have been studied in the present work. These values are smaller than the ramp rate of Section Comparision of Interferometry, Schlieren and Shadowgraph in a Crystal Growth Experiment; consequently the stratification of the solution seen in those experiments was considerably delayed. The rpm of rotational motion fixes the degree of homogenization of the solution and hence, indicates a reduction in the strength of buoyant convection. Crystal rpm of 0 and 15 are studied through experiments. These values have been selected on the basis of their ability to permit growth of crystals of meaningful quality. The effects of ramp rate of the solution, crystal rotation and the size of the growing crystal have been correlated with the growth rate of the crystal. Results of the transient evolution of the convective field in the growth chamber in the form of two-dimensional schlieren images are reported. The images are quantitatively interpreted in terms of concentration contour maps and concentration gradient profiles. In order to bring out the influence of the process parameters, results have been presented in the following sequence: 1. convection currents at a ramp rate of $0.05°C/hour$ with rotations of 0 and 15 rpm; 2. convection currents at a ramp rate of $0.1°C/hour$ with rotations of 0 and 15 rpm; and 3. effect of crystal size.

The nature of fluid motion around the crystal gives rise to $boudary-layers$ in the flow and solutal concentration fields. These are relatively thin zones adjacent to the crystal faces where large changes in velocity and concentration take place. Large concentration gradients are revealed in a schlieren image as a brightened region against a darker background. The images discussed in the following sections show that the stable growth regime of crystal growth is accompanied by thin high intensity zones that originate at the crystal surface. Thus, it is clear that fluid motion and transport occur in the bulk of the solution, but are governed by the physical conditions imposed by the crystal. These are 1. a prescription of fluid velocity in terms of crystal rpm, and 2. concentration levels fixed by salt depletion from the aqueous solution.

Previous Next

RAMP RATE OF $0.05°C/hour$

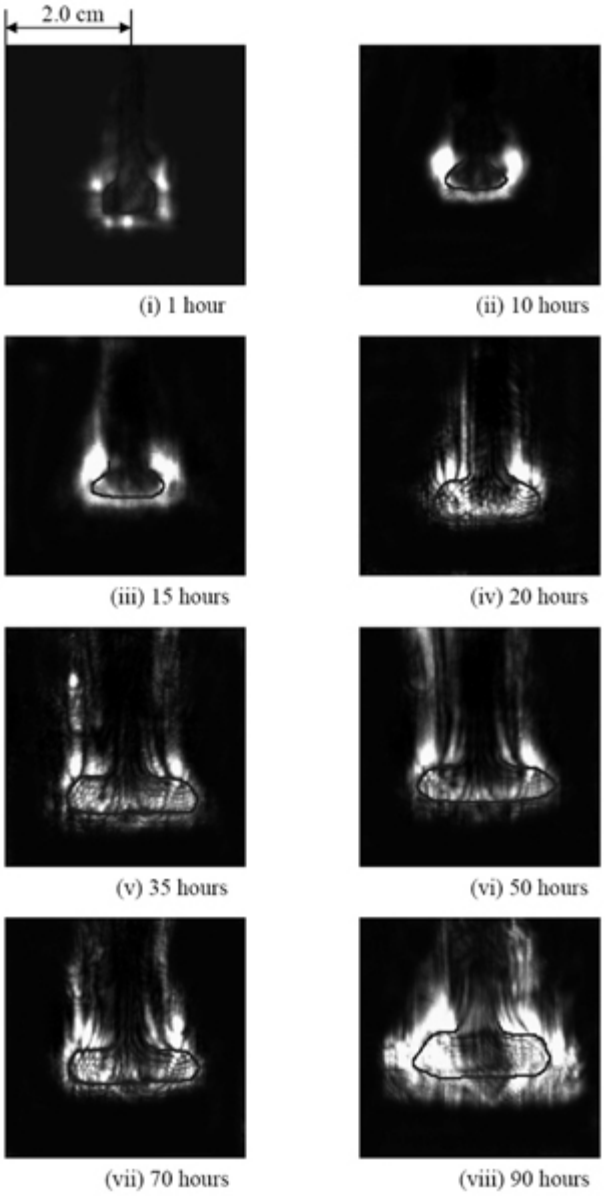

Figure 5.19: Schlieren images of the transient evolution of the convective field around crystal growing from its aqueous solution. (Ramp rate= $0.05°C/hour$, rate of crystal rotation=0 rpm).

Previous Next

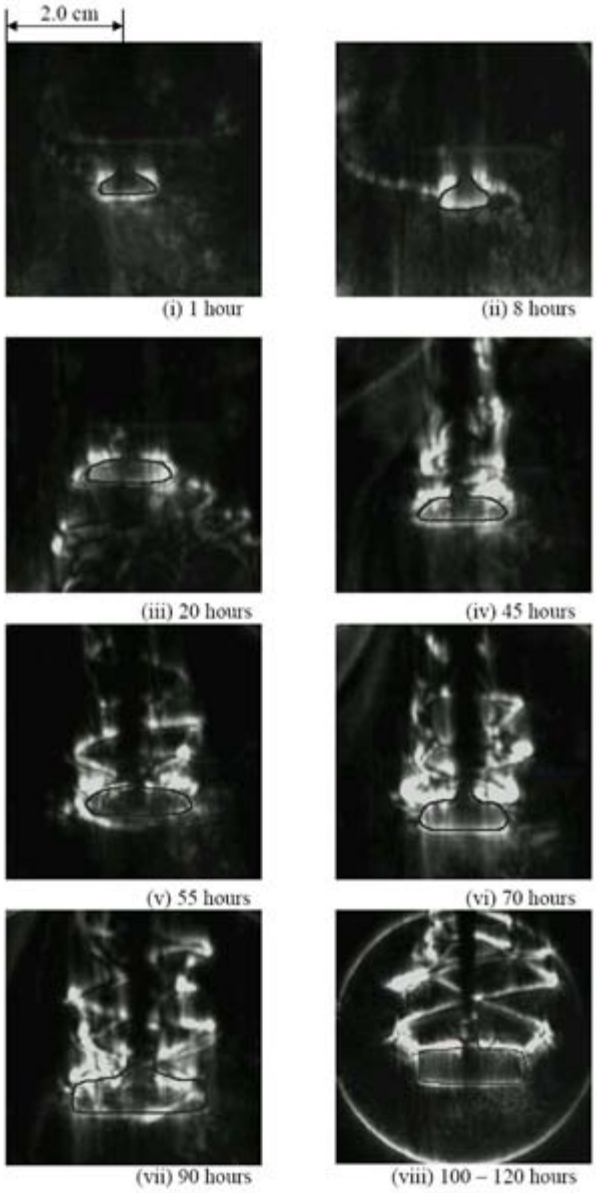

Figure 5.20: Schlieren images of the transient evolution of the convective field around a rotating crystal growing form its aqueous solution. (Ramp rate= $0.05°C/hour$, rate of crystal rotation=15 rpm)

Previous Next

Figure 5.19 and Figure 5.20 show the transient evolution of the convective field for experiments when the growing crystal is respectively held stationary in the solution and rotated at a constant speed of 15 rpm. The ramp rate to cool the solution in the two sets of experiments is $0.05°C/hour$. Insertion of the seed into its supersaturated solution can lead to an instantaneous temperature difference between them, followed by an initial dissolution of the crystal. This phase of the experiment is not included in the figures. With the passage of time, thermal equilibrium is established, and density differences within the solution are solely due to concentration differences. Adjacent to the crystal, the deposition of solute from the solution to the crystal surfaces results in a change of concentration and the solution goes from supersaturated to the saturated state. In the absence of rotation, the denser solution displaces lighter solution in the vicinity of the crystal and a circulation pattern is set up around the crystal. The fluid motion is largely in the vertical plane. With rotation, a radial pressure gradient creates an independent circulation loop that forms an alternative basis of solute movement. Here, the fluid particles around the crystal move in the radial direction, but conservation of mass ensures that vertical velocities be set-up once again. In the purely buoyancy-driven mode (0 rpm; also called *natural convection*), the strength and orientation of the convection currents is determined by the available concentration difference in the solution at any instant of time, and hence the cooling rate. On the other hand, an externally imparted rotation to the growing crystal (called *forced convection*) leads to homogenization of the solution, reduction in concentration gradients and hence a reduction in the strength of convection currents. Except for the initial stages of the growth process (where it is diffusion-dominated), these circulation patterns and their interaction form the basis of the transport of solute from the bulk of the solution to the growing crystal surfaces.

Figure 5.19 shows the sequence of convection patterns in the purely buoyancy-driven mode. Growth in the initial stages of the experiments is accompanied by steady, weak convection, during which diffusion effects can be expected to be significant. Thus, for t = 20 hours, a slow growth of the crystal is to be expected. Concentration gradients are primarily localized in the vicinity of the growing crystal. With the passage of time, the size of the crystal increases, and the gradients grow in strength. This result is brought out in the schlieren images as an increase in the light intensity around the crystal. As defined by the bright region, the resulting flow creates a strong plume directly above the growing crystal. Over a longer period of time (20-90 hours), the plume structure remains unchanged. It indicates a stable growth regime for the crystal, where the buoyant plumes are steady and uniform in nature (Figure 5.19(v-vii)). A gradual evolution of the concentration gradients and the associated buoyant plumes ensure a relatively uniform concentration field in the vicinity of the growing crystal, thus leading to symmetric growth of the crystal at the greatest possible rate. As the crystal increases in size, the convection currents grow in strength. Beyond 90 hours, they are seen to become quite vigorous (Figure 5.19(viii)). Correspondingly, time-dependent movement of the plumes was seen in the experiments. This stage is characterized by local changes in the concentration gradients in the vicinity of the growing crystal, followed by a breakdown in the symmetry of the growth process. It is a limit on the time duration up to which a single growth experiment can be carried out in free convection regime, and the consequent limit on the size of the grown crystal.

Previous Next

The intensity contrast in the images of Figure 5.19, as well as their average intensity progressively increases with time, indicating a depletion of the salt in the aqueous solution. For long times, a stable stratification in density (and hence salt concentration) was obtained in the growth chamber. The rate of increase of the crystal size was negligible at this stage.

Figure 5.20 shows the transient evolution of the convective field around a rotating crystal when the rpm is 15. The first image (Figure 5.20(i)) shows the existence of a diffusion boundary layer around the surfaces of the seed crystal, as seen by the almost uniform distribution of intensity all over the growing faces. After a growth period of about 10 hours, the gradients near the crystal increase in strength. There is a tendency for the plumes to rise vertically, demonstrating that buoyancy forces are larger than centrifugal, on an average. Unlike the schlieren images in Figure 5.19 where the buoyant plume moved almost symmetrically along the seed holder over a considerable part of the growth phase, the images shown in Figure 5.20(ii-iii) reflected temporary unsteadiness in the experiments and asymmetric behavior of the convection currents on either side of the crystal. The unsteadiness can be attributed to two factors: (a) temporary unsteadiness in convection due to the development of prismatic faces from the seed crystal, and (b) the dominance of centrifugal force over the buoyancy force due to crystal rotation, causing the convection currents to be pushed sideways (Figure 5.20(iii)). At all subsequent time periods, the combined effect of buoyancy and rotational forces govern the overall orientation and movement of the convection currents. As the crystal size increases, relatively stronger convection currents rising upwards due to buoyancy lead to stronger concentration gradients near its surfaces. The effective movement of the fluid particles is along a helical path, seen in Figures 5.20(iv-vii), but most clearly in Figure 5.20(vii). The width of the helical structure of the rising plumes scales well with the horizontal dimension of the growing crystal. The increasing strength of buoyant convection is evident from the vertical extent upto which the well-defined helical shape is preserved above the crystal. For example, the respective images for 45 hours (Figure 5.20(iv)) and 55 hours (Figure 5.20(v)) show a breakdown of helical structure in the central region between the upper face of the crystal and the free surface of the solution. Helical symmetry is preserved for the greatest vertical extent (i.e., the distance between the crystal and the free surface of the solution) during the time interval of 90-120 hours (Figures 5.20(vii-viii)). Hence, at a certain level of supersaturation and crystal size, a delicate balance exists between the rotational and buoyancy forces. The balance provides a geometric pattern to the plume, and hence favorable conditions required for the growth of good quality crystals from their aqueous solution is obtained. This particular phase of the growth process can be termed as the stable growth regime in which the crystals of highest transparency and symmetry can be grown. Unlike the growth process in purely buoyancy-driven mode, rotation enforces homogenization of concentration gradients around the crystal over the longer duration of experimental run time. Therefore, the possibility of solute stratification as observed in Figure 5.19(viii) (and at later times) is delayed.

Previous Next

Figure 5.20 shows that the convection regime is purely forced for short time, and is governed by crystal rotation (< 8 hours). The stirring effect is to be seen by the streaks of light in the image that spread out deep into the solution. Between 8 and 20 hours, the spread becomes narrower, as buoyancy forces re-direct the plume in the vertical direction. For times greater than 45 hours, the plumes show a swirl component, but are vertically directed. The relative importance of rotation and gravity is governed by the ratio of buoyancy and centrifugal forces. The force ratio can be shown to be proportional to the crystal size; hence buoyancy is the guiding force at later times, when the crystal has become large. However, rotation provides a kinematic condition for fluid motion (in the form of a boundary condition), causing the buoyant plumes to become helical, and hence structured.

Figure 5.21 shows the concentration contour maps (normalized between 0 and unity) around the growing crystal for 0 and 15 rpm.

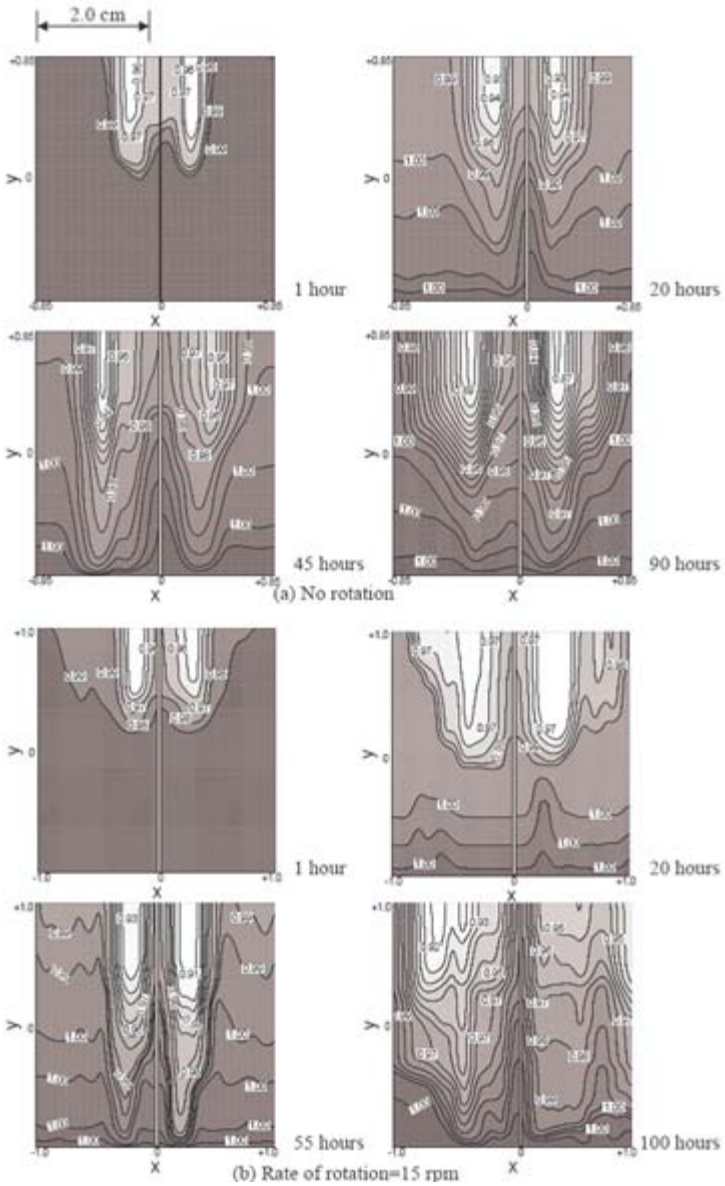

Figure 5.21: Concentration contours around a growing crystal with the passage of time with and without crystal rotation. The central vertical filled band in each plot represents the seed holder. Ramp rate= $0.05°C/hour$

Previous Next

The value of $C = 0$ represents the saturated state, with $C = 1$ being the supersaturated condition at the temperature of the solution in the growth chamber. The maximum crystal size grown in each experiment has been used to non-dimensionalize the x and $y$coordinates. In the following sections, the normalized concentration gradient is based on the ratio of the maximum concentration difference and maximum crystal size. The contours in Figure 5.21(a), corresponding to zero rotation, indicate an almost uniform and symmetric distribution of solute in the growth chamber, both near the crystal and in the bulk of the solution for $t \leq 45$. The contours shown in Figure 5.21(b) also reflect a similar trend over the comparable time period $(t \leq 55\ hours)$. Initially $(t = 1\ hours)$ the contours are localized in the vicinity of the crystal surfaces, with the bulk of the solution being at the supersaturated state $(C = 1)$. This phase of the experiment corresponds to the growth process with transport across a diffusion layer, and correlates well with the schlieren images shown in Figure 5.19 where there is no well-defined upward movement of the buoyant plume. The effect of rotation of the growing crystal can be clearly seen in the contours shown for $1 \leq t \leq 55$ hours, for locations below the crystal $(y = 0)$. While those shown in Figure 5.21(a) (purely buoyancy-driven) depict a larger spread in the upward direction along the seed holder, contours corresponding to 15 rpm are relatively flat. Thus, a uniform distribution of solute is indicated in the solution in the presence of rotation, owing primarily to a mixing action. The vertically rising plume is narrower in the presence of rotation, but broadens with time. At *t*=45 and 90 hours, Figure 5.21(a) shows a slight breakdown in symmetry of the concentration contours below the crystal, with respect to the seed holder, though the plume maintains symmetry. Rotation, on the other hand, enforces a better symmetry to the concentration distribution around the crystal. This is clearly visible at 55 hours in Figure 5.21(b). At 100 hours, the plume is strongly influenced by buoyancy and is as broad as in the case of no rotation. The swirl flow pattern superimposed on buoyant flow by crystal rotation imparts anti-symmetry to the iso-concentration contours. This pattern continues to represent a new form of symmetry for the growth of good quality crystals.

At *t*=20 hours, an asymmetric set of contours is seen in the region below the growing crystal. This temporary asymmetry in the concentration contours is in agreement with the corresponding schlieren image shown in Figure 5.20(iii). It is related to the joint influence of buoyancy and rotation. At other times, either rotation or buoyancy predominates, and symmetry in the concentration distribution is restored.

Previous Next

The growth rate of the crystal is related to concentration gradients, rather than concentration alone. This aspect is explored in Figure 5.22.

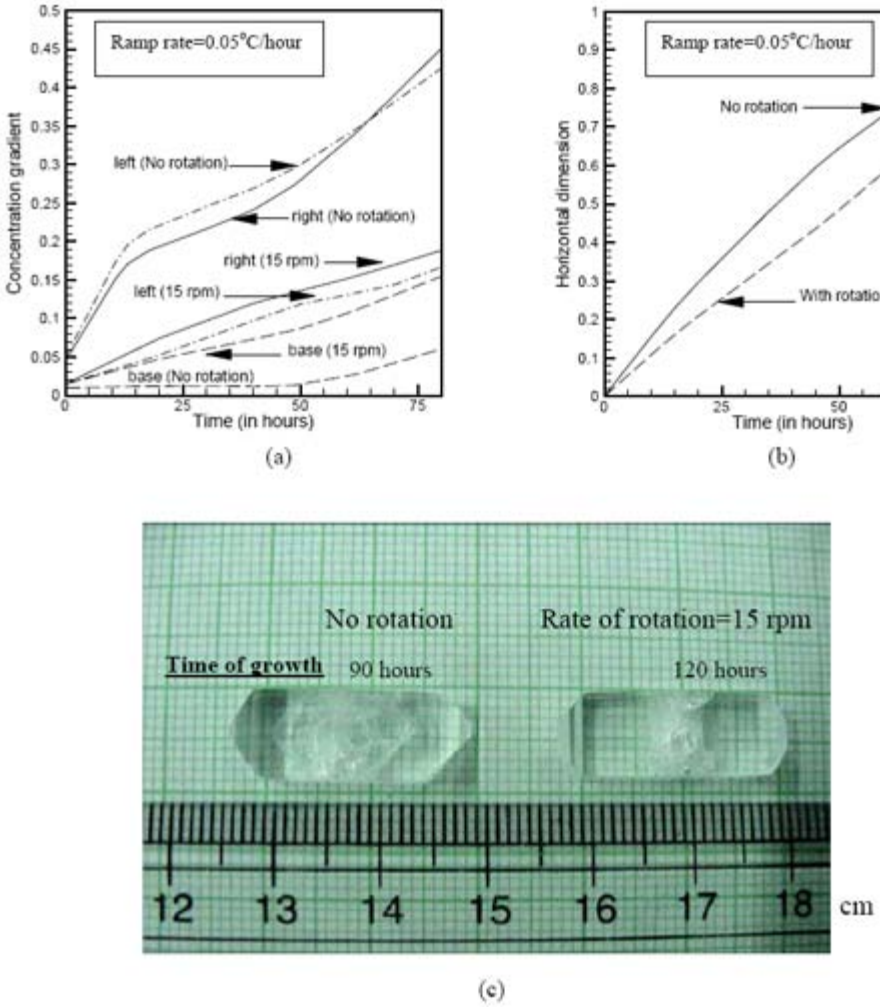

Figure 5.22: (a) Variation of normalized concentration gradients near the three faces of the growing cystal, (b) horizontal growth of the crystal relative to its maximum size as a function of time, and (c) photographs of grown crystals with and without crystal rotation. (Ramp rate= 0.05°C/*hour*)

Previous Next

The variations of the dimensionless concentration gradients averaged over each of the three different faces of the growing crystal (left <001>, right <001> and base <100>) with respect to experimental run time are shown in Figure 5.22(a) for 0 and 15 rpm. As expected, left-right symmetry of the crystal is realized in growth with and without rotation. The effect of rotation is to lower the overall concentration gradient when compared to that generated by buoyancy alone. The gradients on the lower face are small in comparison to the sides. On the lower face, density stratification is stable and buoyant motion is inhibited. The effect of rotation is then to increase the gradients here by inducing fluid movement. Evolutionary profiles on the top face of the crystal are not shown, since the image is adversely influenced by the presence of the seed holder.

In the purely buoyancy-driven experiment, the gradients on the side faces grow in strength with time, whereas the gradients along the lower face are small. The increase in the gradients on the side faces is consistent with the corresponding high intensity regions in the schlieren image sequence shown in Figure 5.19. The problem of high concentration gradients during the later stages of experiments (t = 60 hours) and also a significant difference in the relative distribution of these gradients over sides and lower faces of the growing crystal is seen to be overcome by rotation. The effect of rotation in equalizing the strength of the gradients over the three faces of the crystal is indicated by the proximity of the gradient profiles in Figure 5.22(a). Figure 5.22(b) shows the horizontal growth of the crystal with respect to the experimental run time. The growth rate with rotation is slightly lower when compared to that based on buoyancy alone; it is however practically linear. The growth rate with crystal rotation is comparatively lower because of two factors: (a) the lowering of concentration gradients in the vicinity of the growing crystal $(t \geq 60\ hours)$ due to homogenization of the solution induced by crystal rotation, and (b) the rotation of the crystal introduces a radial (outward) velocity component that inhibits the transport of solute to its growing surfaces. Figure 5.22(c) shows photographs of the grown crystals for the two cases. The size of the finally grown crystal (after 90 hours) is larger in buoyancy-driven convection, but the crystal quality is superior in terms of transparency when growth is accompanied by rotation.

Previous Next

RAMP RATE OF $0.1°C/hour$

When the ramp rate is increased, the amount of salt that is held in the supersaturated solution increases. The consequence is a greater driving potential for buoyant convection. There is an outer limit to the degree of super-saturation of the solution, though it was not reached in the present study. The growth process of a crystal when the solution is cooled at a higher ramp rate of $0.1°C/hour$ is discussed in this section.

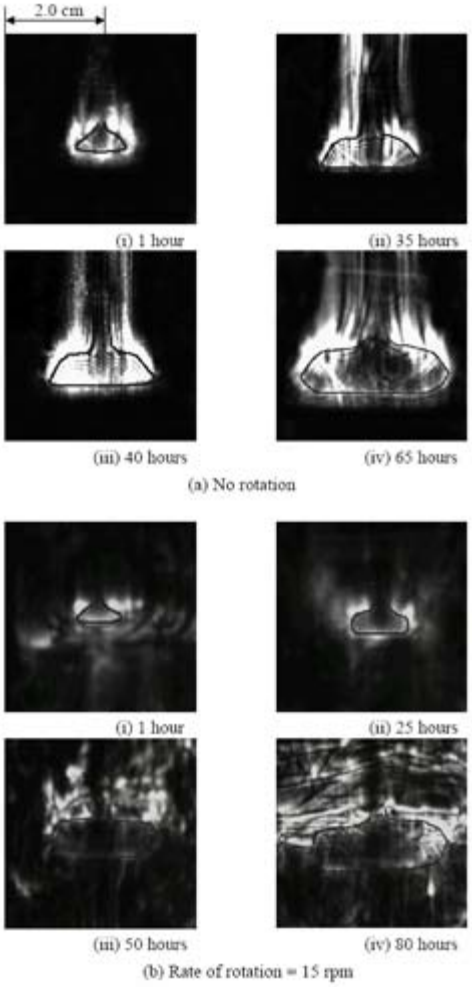

Figure 5.23: Schlieren images of the transient evolution of the convective field around a KDP crystal growing from its aqueous solution with and without crystal rotation. (Ramp rate= $0.1°C/hour$)

Figure 5.23 shows the transient evolution of the convective field in a purely buoyancy-dominated growth regime (0 rpm, 5.23(a)) and under the combined effects of buoyancy and rotation of the crystal (15 rpm, 5.23(b)). In comparison to the sequence shown in Figure 5.19 (ramp rate=$0.05°C/hour$, 0 rpm) the region in the vicinity of the growing crystal reveals a bright intensity distribution, indicating larger concentration gradients in the buoyancy-driven regime. The spread of the bright patch at *t*=1 hour shows that fluid motion has set in quite early. Thus, even the initial growth is not diffusion-controlled. The buoyancy-driven fluid motion is more vigorous at the higher ramp rate, leading to a greater vertical spread of the depleted solution, and a narrower plume. A clear movement of the buoyant plumes on either sides of the seed holder can be seen at *t*=35 hours in Figure 5.23(a), whereas at a comparable time instant, weak convection currents were observed at a lower ramp rate of Figure 5.19. Schlieren images in Figure 5.23(a) show well-defined, strong buoyant plumes that transport solute from the bulk of the solution to the crystal surfaces at a faster rate. Consequently, the crystal size at 65 hours in Figure 23(a) is larger than that at 90 hours in Figure 5.19. Rotation of the growing crystal tends to diminish the high concentration gradients in the growth chamber. It is clearly seen from the schlieren images shown in Figure 5.23(b) for $t \leq 25$ hours. In contrast to pure buoyancy, the convection currents do not rise vertically upwards; instead they are dispersed in the solution as they are determined by the combined effects of buoyancy and rotational forces (Figure 5.23(b), *t*=25 hours). The sizes of the crystal and the convection pattern in the mixed regime (when rotation and buoyancy are of comparable magnitude) are similar in Figures 5.20 and 5.23(b). Furthermore, lower concentration gradients due to the homogenization of the solution are reflected by the weak intensity contrast in Figure 5.23(b) in comparison to that in Figure 5.23(a).

As the crystal size increases, vigorous convection currents in the solution due to buoyancy result in steep concentration gradients around the crystal (Figure 5.23(a), *t*=65 hours). In the presence of rotation (Figure 5.23(b), *t*=50 and 80 hours), the plumes orient themselves in the vertical direction, showing that buoyancy predominates over rotation. However, the flow field is clearly disorganized, leading to the appearance of light streaks that are smeared in the horizontal direction by the circulating flow. There is a considerable loss of symmetry in the concentration field at all time instants. At *t*=80 hours, the higher ramp rate removes a considerable amount of solute from the solution, leading to density stratification in the growth chamber (Figure 5.23(b)). Rotation has no impact on the concentration field at this stage.

Previous Next

In the presence of rotation, the influences of a lower and a higher ramp rate can be discussed as follows. In the former experiment, rotation imparts symmetry of the solute distribution, diminishes the gradients, the crystal growth rate and results in crystals of better transparency. In the latter, rotation has a less significant role. The solute distribution is homogenized, but there is no improvement in the symmetry of the concentration contours. The crystal growth rates remain high and the solution is density stratified in a shorter period of time. The growth of the crystal is halted at this point. The above discussion shows that for a given ramp rate, a judicious choice of crystal rotation can lead to an enhanced crystal quality, though a slower growth process.

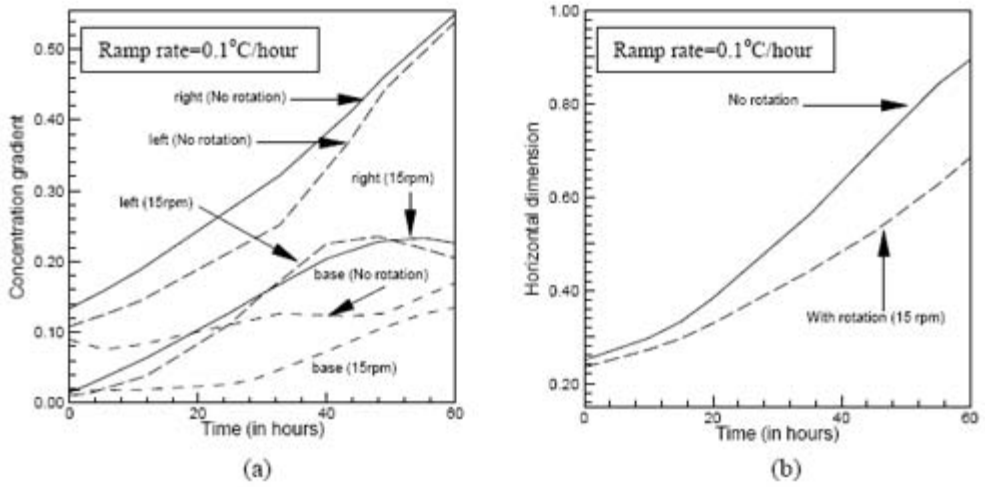

Figure 5.24: (a) Variation of normalized concentration gradients near the three faces of the growing crystal, (b) horizontal growth of the crystal relative to its maximum size as a function of time, and (c) photographs of grown crystals with and without crystal rotation. (Ramp rate= 0.1°C/*hour*)

Figure 5.24(a) shows the evolution of concentration gradients on the faces of the growing crystal for a ramp rate of $0.1°C/hour$. In the purely buoyancy-driven growth regime, the gradients on the side faces of the crystal progressively keep increasing. Thus, very high concentration gradients are obtained towards the late stages of growth. On comparing with the corresponding variation of concentration gradients with time in Figure 5.23(a), the effect of higher ramp rate of the solution can be clearly understood. The maximum non-dimensional value of concentration gradient for the ramp rate of $0.1°C/hour$ is around 0.55 observed at *t*=60 hours. For the lower ramp rate ($0.05°C/hour$), the corresponding value is 0.45 after 80 hours. To some extent, rotation lowers the monotonic increase in the concentration gradients in Figure 5.24(a), and improves the left-right symmetry. The difference is on the lower side, where rotation further diminishes concentration gradients, in comparison to growth without rotation. This result is the reverse of what is seen in Figure 5.22(a). The large gradients on the side faces, and low gradients on the horizontal faces leads to high growth rates of the horizontal dimension of the crystal (Figure 5.24(b)), that is relatively insensitive to rotation. The quality of the grown crystals (Figure 5.24(c)) is inferior in transparency to that obtained with a lower ramp rate ($0.05°C/hour$) that is shown in Figure 5.23(c).

Previous Next